Interferometric Force Probes for Thruster Plume Diagnostics and Indirect Thrust Measurements

IEPC-2017-096

Presented at the 35th International Electric Propulsion Conference
Georgia Institute of Technology – Atlanta, Georgia – USA
October 8–12, 2017

Thomas Trottenberg*, Alexander Spethmann†, and Holger Kersten‡
Institute of Experimental and Applied Physics, University of Kiel, 24098 Kiel, Germany

A probe for the measurement of forces exerted by a thruster plume on a small test surface is described. The force probe is intended for diagnostics of the plumes of electric spacecraft propulsion engines, in particular the determination of the spatial distribution of the momentum flux. The instrument makes use of a sensitive cantilever whose elastic deflection is measured interferometrically. The present paper focuses on setup and calibration of the probe, and the involved errors are discussed. Examples of use of the probe can be found in two other contributions to the proceedings of this conference.

Nomenclature

A	= area of the test surface of the force probe
D	= calibration constant
d	= displacement of the mirror mounted on the cantilever
δ	= displacement of the end of the cantilever
E	= Young's (elastic) modulus
F	= force acting on the test surface
F_{thrust}	= thrust
f	= momentum flux density ("differential thrust")
f_0	= natural frequency of the cantilever
g	= gravitational acceleration
I	= second moment of inertia of the cantilever
$L_{\mathrm{m}}, L_{\mathrm{t}}$	= distance of the mirror and the target centers from the fixed end of the cantilever
λ	= scaling factor in the context of a warming of the cantilever
m	= mass of a calibration weight
r	= radial position in a thruster plume
r_{max}	= radius of the thruster plume
r_1, r_2	= outer and inner radius of the cantilever tube
S	= stiffness of the cantilever
T	= temperature of the cantilever
ΔT	= change of the cantilever temperature
t	= time
τ	= damping time constant for the natural frequency of the cantilever

*Research Associate, Plasma Technology, trottenberg@physik.uni-kiel.de
†Research Associate and doctoral candidate, Plasma Technology, spethmann@physik.uni-kiel.de
‡Professor, Plasma Technology, kersten@physik.uni-kiel.de

I. Introduction

DIAGNOSTICS for exhaust plumes of electric spacecraft propulsion engines are often based on electric probes like Faraday cups[1] and retarding field analyzers.[2] Less frequently, spectroscopic techniques like optical emission spectroscopy,[3] laser absorption spectroscopy[4] and laser-induced fluorescence[5] are applied. Recently, momentum flux measurements, i.e. force measurements, were performed in the beam of an industrial broad-beam ion source that is very similar to the plume of gridded ion thrusters.[6] An advantage of this novel force measuring approach over the standard electric methods results from the fact that the latter are sensitive only for the charged species. In contrast, force probes do not discriminate between charged and neutral energetic particles. This is an important issue because thruster plumes often contain a non-negligible amount of energetic neutral atoms, which can also be involved in the generation of thrust.[7] Moreover, additional energetic neutral atoms can originate from charge-exchange collisions with the gas behind the exhaust that unintentionally escapes from the thruster and with remaining gas in the test chamber.

In this contribution, we describe a technique for the measurement of forces exerted by a thruster plume on a small test surface. In comparison with our formerly reported force measurements that used electromagnetically compensated pendula,[6,8–10] the here presented probe is based on a sensitive elastic cantilever whose deflection is measured interferometrically. At the IEPC two years ago, we already presented a first implementation of this measurement principle.[11] In that case, the displacements were even measured along two independent (orthogonal) axes, whereas the present paper describes a probe that records only the force component perpendicular to the test surface. For most of the plume diagnostic applications, the measurement of the component along the expected thrust vector of the engine will be sufficient. Since 2015, further progress in the development of the probe was made within a project funded by the German Aerospace Center (DLR). This proceeding paper summarizes the state of the development at the end of the funding period.

Scanning a cross section of a thruster plume yields information about the momentum distribution in the plume. The measured "differential thrust" at a specific point in the plume, i.e. the spatially resolved momentum flux density or force per area, is obviously valuable information for improvements of the thruster.[12] On the other hand, an integration of the locally measured momentum flux density over the entire cross section yields the thrust vector of the engine, so that the force probe becomes an indirectly measuring thrust balance. In case of very small engines, e.g. field-emission electric propulsion thrusters, the target could even collect the entire plume and determine the thrust by a single measurement.[13]

II. Description of the probe

The force probe uses a thin ceramic tube as an elastic cantilever (see Fig. 1). A small circular test surface with a diameter of 20 mm is mounted at the free end of the ceramic tube. The aluminum target holder is connected to a wire that is fed through the tube; in case of a conductive target, it serves for biasing and measurement of the current taken by the test surface. The real target is clamped to the holder by means of thin straps, which extend radially from the circular target surface and are folded around the edge of the holder plate. When a force acts on the test surface, the tube is elastically bent (not more than a few micrometers), so that each point of the cantilever is minimally displaced from its initial position. In terms of the theory of elasticity, the cantilever is essentially a cylindrical beam with one fixed end. The displacement of a specific part of the cantilever serves as the quantity to be measured. In order to determine the deflection, an interferometric displacement sensor is used, which measures the displacement of a small mirror attached to the cantilever. The mirror is accomplished by the polished surface of a stainless steel cuboid with a bore of the same radius as of the ceramic tube.

A. Displacement sensor

The interferometric displacement sensor is a commercial product (attoFPS 3010) from the Attocube Systems AG, Germany,[14,15] which applies the frequency-modulation continuous wave (FMCW) interferometer method.[16] It uses the path between a plane fiber end and a mirror as cavity, where a lens is placed between fiber and mirror that expands the light to a thin beam of parallel rays. A few percent of the 1550 nm laser light (150 μW) are reflected backwards at the plane end of the fiber and serve as the reference wave, while most of the light leaves the fiber and reaches the mirror. The light reflected at the mirror could directly re-enter the fiber through the same plane end and finally interfere with the reference wave at the detector outside the vacuum chamber at the other end of the wave guide. However, this *single-path* technique has two

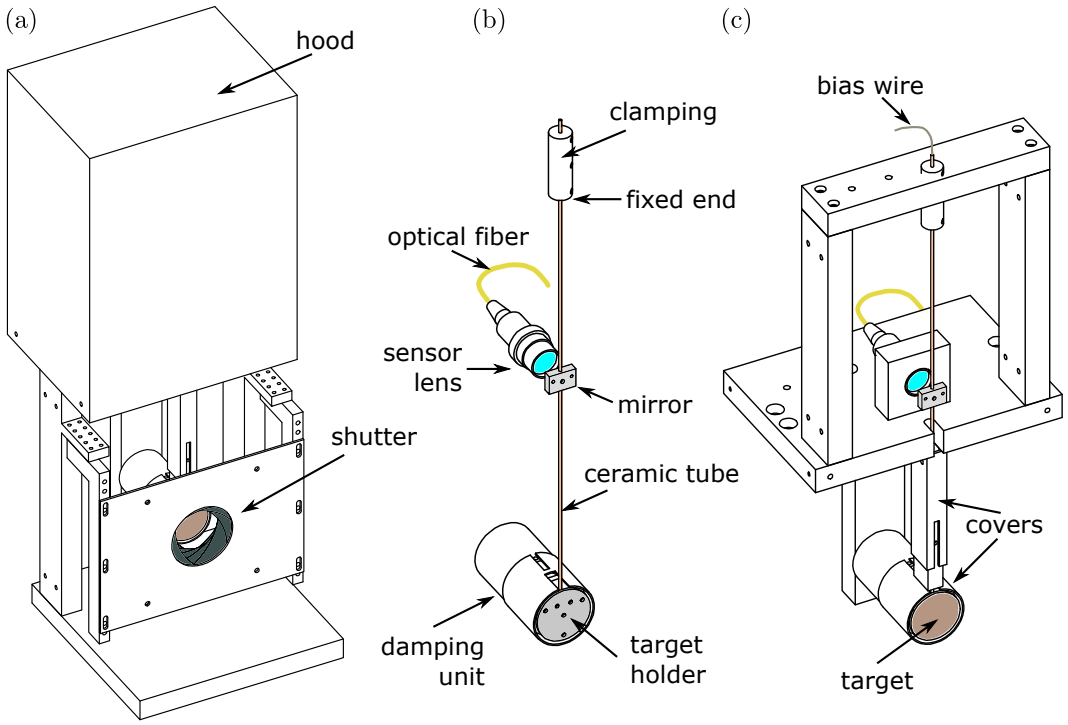

Figure 1. Implementation of the force probe. (a) Probe with the optional shutter und the protective hood, (b) all essential parts of the probe, (c) necessary mechanical structures of the setup.

disadvantages: first, the mirror has to be aligned very precisely in order to receive and reflect the light rays perpendicularly, and second, the wave coming from the mirror has a much higher intensity than the reference wave. Therefore, the signal contrast would be low and the displacements might not be detectable. For this reason, the wave from the mirror is attenuated by the *dual-path* method: The mirror is slightly tilted ($< 1°$), so that the returning light is not focused on the fiber core. The focal point has now a small lateral shift and lies on the front surface of the zirconia ferrule of the fiber connector. From there, the light is strayed and significantly attenuated. A part of the light is collimated by the lens and passes the cavity once again in both directions. Note, that this second half of the path coincides automatically with the first one. Finally, the light is focused right at the fiber core, where it re-enters the fiber. The alignment in the dual-path method is much more robust than in the single-path method because of the 'self-aligning' effect: The final focal point is right at the point from where the light emerged. This patented technique was described and investigated in detail by Thurner, Braun, and Karrai.[14]

A conventional Fabry-Pérot interferometer has the two drawbacks of, firstly, low sensitivity sensing spots at the interference extrema and, secondly, the ambiguity of the displacement direction. Therefore, this interferometer modulates the laser wavelength periodically with a frequency of 12.5 MHz.[15–17] The use of optical fibers and vacuum feedthroughs allows to keep the cavity length short and to have the electronic parts outside the vacuum chamber.

B. Mechanics

The masses of the target assembly (2.3 g), the mirror (1.5 g), and the ceramic tube with the wire give rise to undesired mechanical oscillations. In particular, vacuum pumps for test chambers always excite eigenmodes; but also an abrupt change of the force that is to be measured would cause a ballistic overshoot beyond the equilibrium position and subsequent weakly damped oscillations. A finite element modal analysis of a slightly simplified model of the moving masses revealed that there are two modes to be expected at the frequency of 9.0 Hz. These two modes are in-phase oscillations at which the mirror and the target move in the same direction; one mode is normal to the target, and the other one is parallel to it. The next higher calculated mode pair occurs at 73 Hz and corresponds to anti-phase oscillations of the mirror and the target.

Figure 2 shows a modal analysis of measured displacements of the mirror. The sampling rate of the

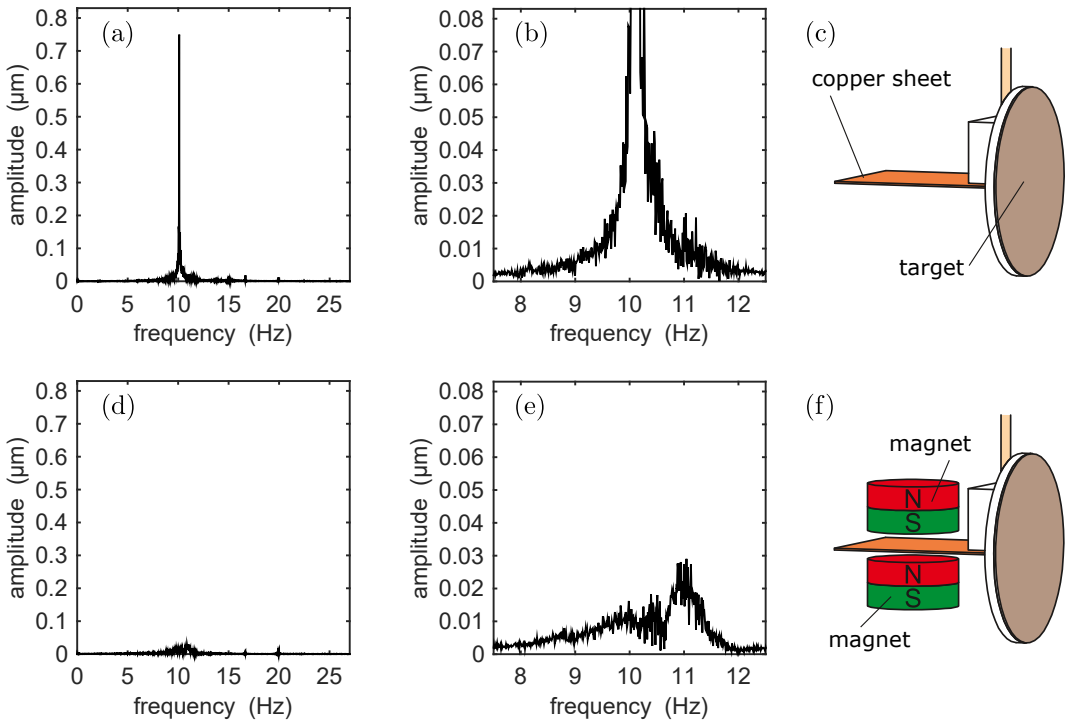

Figure 2. Mechanical oscillations of the cantilever and its damping. (a) Frequency spectra of the oscillations without damping and (b) an enlarged plot of the same data centered about the natural frequency. (c) The target assembly prepared with the copper sheet for the eddy current damping (configuration without damping). (d) Spectra of the oscillation with damping and (e) an enlarged plot of the same data centered about the natural frequency. (f) The target assembly with the magnet pair of the eddy current unit (configuration with damping).

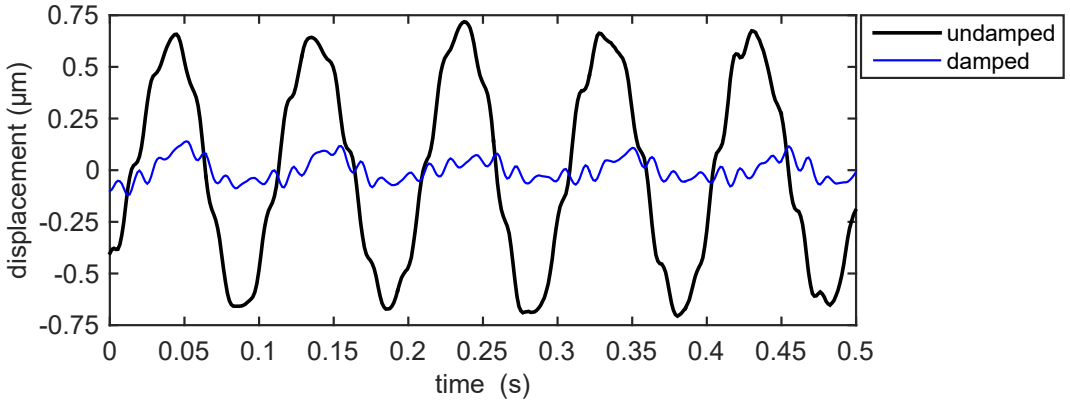

Figure 3. Mechanical noise. The time series show the recorded oscillations of the mirror (a) without and (b) with the eddy current damping unit. The measurement is performed in a common lab environment without further provisions for vibration absorption.

displacement sensors, 1.5 kHz, is much faster than the frequencies of the expected mechanical modes. The probe is placed on a laboratory table without special damping provisions for this test measurement. The corresponding time series in Fig. 3 displays half a second of the series (denoted as "undamped"). The oscillations extend to $\pm 0.75\,\mu$m. The frequency analysis (absolute values of the discrete Fourier transforms) of the in total 50 s long time series of the displacements is shown in Fig. 2(a); it exhibits one distinct peak at $f_0 = (10.1 \pm 0.1)$ Hz. With the exception of a very small peak at 67 Hz (amplitude $0.04\,\mu$m), no significant signals are found beyond 25 Hz.

The vibrations at the natural frequency f_0 do not constitute a serious drawback for force measurements as long as the displacements caused by the force are not too small in comparison with the mechanical noise. Averaging over several periods of the natural frequency reduces the noise.

C. Eddy current damping

In order to keep the required sampling time short, the probe is equipped with a damping mechanism. Figures 2 (c) and (f) show the essential parts of the eddy current damping unit. A pair of small cylindrical permanent magnets provides a magnetic field that penetrates a thin copper sheet attached to the back side of the target holder. The target together with the copper sheet oscillates perpendicularly to the field lines, so that eddy currents are generated in the sheet. The currents create a counteracting force (Lenz's law) and dissipate energy stemming from the oscillation. Figure 3 shows the time series of the measured displacements for the damped and the undampled case. The oscillations are significantly reduced. This can also be seen in the spectrum in Fig. 2 (d). Interestingly, there persist modes about 11 Hz, which is better displayed in the enlargement in Fig. 2 (d). These 11 Hz modes are also present in the undamped case, see Fig. 2 (b). The remaining modes must stem from the entire setup that is not affected by the damping mechanism: Vibrations of the lens are also detected as displacements, and vibrations of the damping unit itself are even unintentionally transmitted to the target via the eddy currents.

Figures 4 (a) shows the response of the undamped probe to a strong pulse. The pulse was caused by cautiously knocking on the laboratory table. The amplitude of the f_0 mode decays exponentially with a time constant of $\tau = 13$ s, i.e. $\propto \exp(-t/\tau)$ for t counted from the beginning of the decaying perturbance. The response with the eddy current damping mechanism is displayed in Fig. 4 (b). Now, the damping time is reduced to $\tau = 0.5$ s.

The measurements require a reference displacement for the case without the force that is to be determined. These reference measurements are performed shortly before or after the main measurement with the force. This method ensures that temporal mechanical changes of the experimental setup are not misinterpreted as forces. In electric propulsion test chambers for example, diagnostics are usually mounted on mechanical structures that are exposed to the truster plume. The structures are unintentionally heated, which gives rise to small displacements. Thus, the gravity vector could slightly be tilted relative to the probe, so that the cantilever with the masses of the target and mirror assemblies adopts a different equilibrium position that would be detected as a displacement. Such drifts occur at time scales much longer than a measurement, which can be performed within a few seconds, and become negligible when reference measurements are performed shortly before or after the main measurement.

D. Beam shutter

Finally, we introduce an optional component that becomes necessary for measurements in environments where it is not feasible to repeatedly switch the beam on and off for the reference measurements. For this purpose, a beam shutter is placed directly in front of the probe target (see Fig. 1). The shutter consists basically of a blade iris that has a maximum aperture of 36 mm and can be closed completely. A small direct-current motor drives the blades for quick opening and closing. Measurements in the plume of a Hall thruster have recently been performed with the beam shutter and are presented in another IEPC proceedings paper.[12]

E. Target material

The target is preferably made of a material with low sputter yield. In case of sputtering at the test surface, it has to be taken into account that the released particles, which are sputtered atoms from the target and re-emitted atoms from the propellant, contribute to the momentum balance. These effects have been

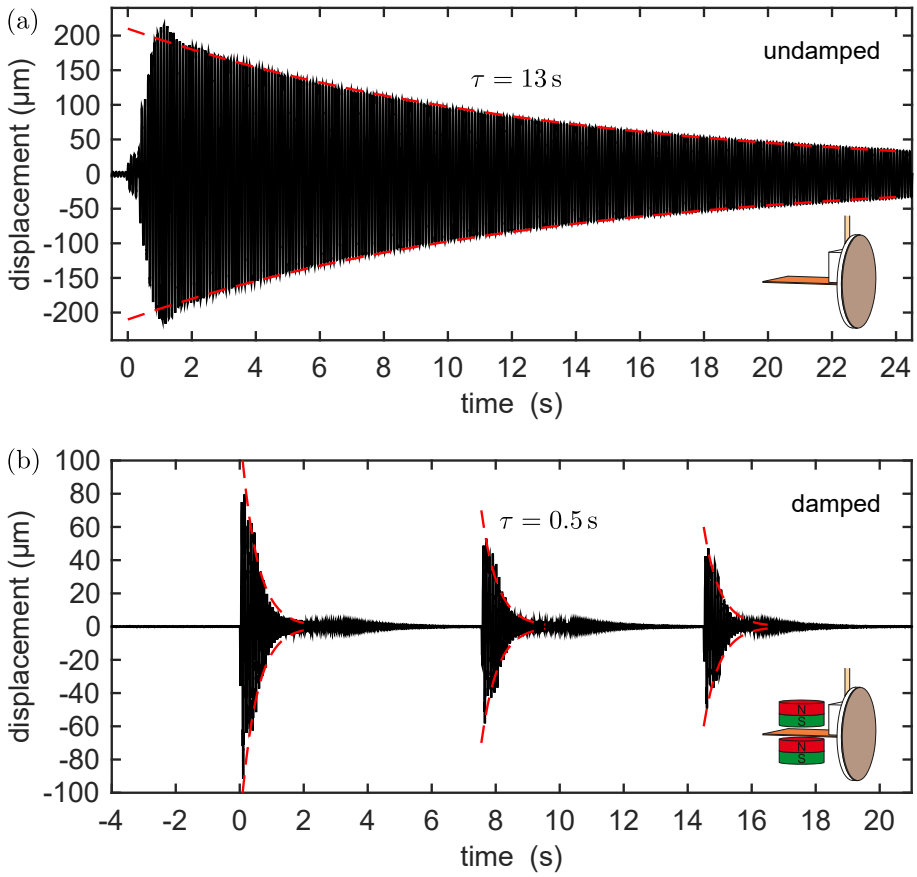

Figure 4. Decay of the oscillations caused by mechanical shocks, (a) without and (b) with the eddy current damping unit. The damping time constant τ is significantly reduced by the damping mechanism.

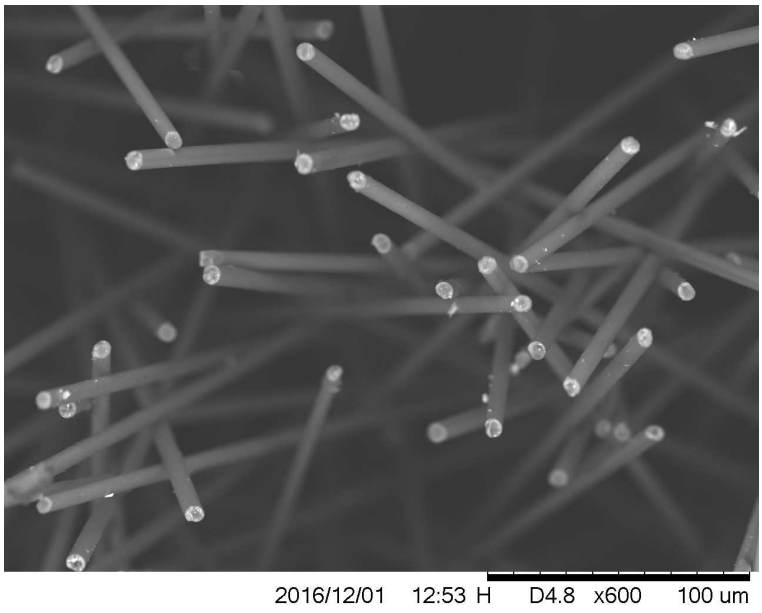

Figure 5. Scanning electron microscopy image of the carbon fiber velvet.

studied by means of specially designed force probes,[10,18–20] and the results have been reported at IEPC conferences,[12,21,22] too. For example, in case of a copper target and perpendicularly impinging Ar particles with kinetic energies of 1220 eV, the measured force was found to be 36% larger than the momentum flux carried by the beam particles that hit the target.[12,18]

In contrast to copper, a perfectly absorbing and not sputtering material would experience a force that corresponds exactly to the momentum flux of the impinging particles. Carbon has a low sputtering yield, and graphite is therefore often used for beam dumps in test chambers. The experimental results show that graphite yields forces that are indeed very similar to the forces expected from a perfect absorber.[12,18] However, the effective sputter yields can be reduced even more when a highly porous material is used. "Carbon fiber velvet" (produced by the Energy Science Laboratories, Inc.) is such a material; it consists of approximately 2.2 mm long and 7 μm thin carbon fibers that are attached with one end at a plane base. Figure 5 shows a scanning electron microscopy image of the fibers. The geometry allows the ions to enter deeply into the porous material. Consequently, carbon that is sputtered in its inner will be re-deposited somewhere at other fibers in the material. Beam atoms very likely undergo more than one contact with the fibers before they leave the material with significantly reduced energy and momentum. The already mentioned studies of forces that are generated when a surface is sputtered reveal that the carbon fiber velvet is an even better absorber than graphite.[12,18]

III. Calibration and Errors

For a calibration, the instrument is laid on its rear side so that certified milligram weights can be put on the test surface. We use in this case only the mass $m = 10\,\mathrm{mg}$ ($\pm 0.006\,\mathrm{mg}$), where the weight is put and removed 10 times on the test surface in order to obtain also reference measurements without the weight. The force $F = mg$ is calculated using the local gravitational acceleration $g = 9.81\,\mathrm{ms}^{-2}$. The weight is put always on the center of the test surface, which is important and will become clear from the theoretical consideration below. We obtain the calibration constant $D = (22.1 \pm 0.1)\,\mu\mathrm{N}\,\mu\mathrm{m}^{-1}$.

The following estimation confirms the order of magnitude of the calibration constant. The underlying theory of the deformation of solids can be found in many textbooks, e.g. Ref. 23. The cantilever is a tube with an outer radius of $r_1 = 0.5\,\mathrm{mm}$ and an inner radius of $r_2 = 0.25\,\mathrm{mm}$. The mirror and the target centers are at the distances $L_\mathrm{m} = 75\,\mathrm{mm}$ and $L_\mathrm{t} = 175\,\mathrm{mm}$ from the fixed end, respectively.

The stiffness $S = F/\delta$ describes the deflection δ of the free end under the action of the force F at the free end as a special case of Hook's law. The stiffness of the beam

$$S = \frac{2EI}{L_\mathrm{t}^3} \tag{1}$$

can be calculated from Young's modulus E, and I is the second moment of area of the cantilever cross-section for the direction of the bending. In case of the tube geometry of the ceramic cantilever, one finds

$$I = \frac{\pi}{4}(r_1^4 - r_2^4) \quad , \tag{2}$$

which is the same for all bending directions because of the rotational symmetry of the cross section. Note that not the deflection at the free end, where the target is mounted, is measured but the deflection d at the position L_m of the mirrors. The deflection at this specific position on the beam can also be calculated,[23] and the deflection-to-force conversion factor $D = F/d$ becomes

$$D = \frac{F}{d} = \frac{6EI}{L_\mathrm{m}^2(3L_\mathrm{t} - L_\mathrm{m})} \quad . \tag{3}$$

Assuming an elastic modulus $E = 3.09 \times 10^{11}\,\mathrm{Pa}$ for the Al_2O_3 ceramic at room temperature,[24] one would expect $D = 33.7\,\mu\mathrm{N}\,\mu\mathrm{m}^{-1}$. This is the same order of magnitude, but the measured value is about 1/3 smaller. One part of the difference can be attributed to the tolerance in the radii ($\pm 5\%$) on which D strongly depends, see Eq. (2). Furthermore, the elasticity of the polycrystalline material is only imprecisely known, since the elastic modulus E depends on purity, size of the crystallites, and the porosity, which all result from the manufacturing method.

Finally, we discuss the influence of the cantilever temperature T on the deflection-to-force conversion factor. Young's modulus $E(T)$ of the alumina specimen investigated in the above mentioned study[24] decreased linearly with increasing temperatures $T < 900\,^\circ\mathrm{C}$, and a plot in that publication shows a negative

slope of approximately $\mathrm{d}E/\mathrm{d}T = -4 \times 10^7\,\mathrm{Pa\,K^{-1}}$. A temperature rise of $\Delta T = +100\,\mathrm{K}$ starting from room temperature (293 K) lowers E by 1.3% ($E = 3.05 \times 10^{11}\,\mathrm{Pa}$), and the calibration constant D decreases consequently by 1.3%, too. When a significant warming of the cantilever is expected, this effect should be considered.

There is a simple way how a changing "spring constant" D could be monitored without additional temperature sensors, which obviously should not be attached to the cantilever. However, this technique works only when the damping unit is not used, because it relies on an evaluation of small shifts of the natural frequency f_0. For an ideal beam with one free end and no additional masses attached to it, the square of the natural frequency f_0 is proportional to Young's modulus E, i.e. $f_0^2 \propto E$. One can easily reason that this holds for the geometrically more complicated force probe cantilever as well, since the elastic modulus E still enters linearly in all the forces that move the cantilever. Hence, an increase of E by a factor of λ makes the motion by the factor λ^2 faster (time scales proportionally to λ^{-2}), i.e. frequencies of oscillations would increase by the factor λ^2. This is confirmed by the above mentioned finite element modal analysis that results in a decrease from 8.97 Hz to 8.91 Hz (exactly −0.65%) for the first two modes, when the temperature rises by $\Delta T = +100\,\mathrm{K}$ from room temperature. The finite element stationary solution for the deformation caused by a constant force yields a change of the calibration constant from $32.2\,\mu\mathrm{N\,\mu m^{-1}}$ to $31.7\,\mu\mathrm{N\,\mu m^{-1}}$, i.e. a decrease of 1.3%, which confirms the above estimation.

A by 1% ($\lambda = 0.99$) lower frequency f_0 would indicate a by 2% ($\lambda^2 = 0.98$) smaller conversion factor D, which would certainly still be a negligible error for most applications. However, such a small frequency drift, for example from $f_0 = (10.1 \pm 0.1)\,\mathrm{Hz}$ to $(10.0 \pm 0.1)\,\mathrm{Hz}$, could barely be detectable, see Fig. 2.

IV. Measurement procedure

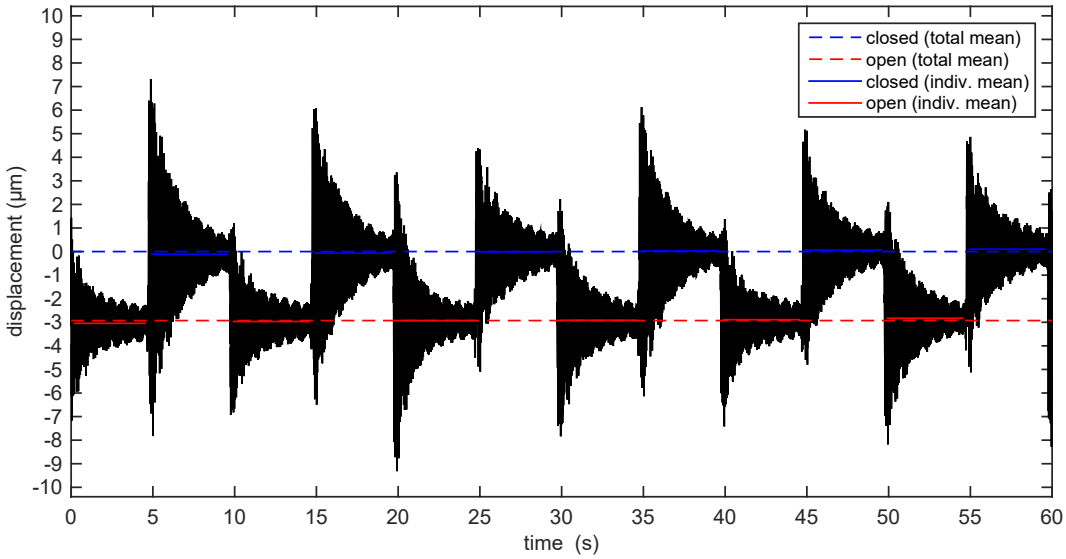

Figure 6. Time series of the measured displacements using the beam shutter. The forces are generated by a 1.2 keV Ar beam from a broad beam ion source. The probe is equipped with a carbon fiber velvet target with an area of $A = 3.14\,\mathrm{cm^2}$. The red and blue dashed and solid lines indicate time averages corresponding to the intervals over which they extend.

We demonstrate the measurement procedure in a test environment, where a 1.2 keV Ar beam is generated by a microwave broad beam ion source.[12,18] The probe is placed at a distance of approximately 90 cm from the ion source. The target material is the above described carbon fiber velvet, and the eddy current damping unit is installed. The shutter is programmed to alternate beam exposure times of 5 s (shutter opened) and 5 s with the closed shutter.

The time series in Fig. 6 shows the displacements. One notices the overshooting at the switching times and the subsequent damped oscillations. For the determination of the displacements in the individual periods of time, the respective averages are calculated (the data closer than 0.2 s to the switching time points were excluded from the averaging). The average displacements are indicated in Fig. 6 by horizontal lines. The

solid lines are for the averages in one of the individual 5 s intervals, respectively, whereas the two dashed lines represent the averages over all six on and off times, respectively.

The average displacement is $d = -2.93\,\mu$m, corresponding to a force of $F = 64.7\,\mu$N. (Negative displacements mean a shortening of the distance between lens and mirror.) The standard deviation of the twelve individual measurements is $\Delta d = 0.07\,\mu$m, corresponding to a standard deviation $\Delta F = 1.6\,\mu$N of the individual force measurement. This can be interpreted as a relative error of 2.5% for this force measurement.

V. Conclusion

This paper presented an instrument for the measurement of momentum fluxes in the plume of an electric space propulsion engine. The functional principle is based on an elastically bendable cantilever with one fixed end and a test surface mounted at the free end. The deflection of the cantilever is measured with an interferometric displacement sensor. A mirror is attached to the cantilever between the free and the fixed end in order to reflect the laser light from the optical sensor. The displacements of the test surface are recorded at a sampling rate faster than 1 kHz.

Typical deflections are in the order of magnitude of a few micrometers, corresponding to some tens of micronewtons. The Fabry-Pérot type interferometer setup uses one fiber optic, which allows that only the small cavity parts have to be integrated in the probe. The laser and the data acquisition electronics are operated outside the vacuum chamber.

The calibration is performed by putting one or more small weights directly on the test surface. For this purpose, the cantilever and the test surface are horizontally oriented, so that the weights act in the direction of the surface normal.

It is found that the errors of a force measurement are mainly determined by the mechanical noise, which is generated in particular by vacuum pumps. By this environmental noise, mainly the mode at the natural frequency in the order of magnitude of 10 Hz is excited. It is possible to measure forces smaller than the noise level by means of averaging the measured time series, but this requires longer measurement times. A damping mechanism based on eddy currents was described. By this method, the modes at the natural frequency can be damped very efficiently.

Furthermore, a beam shutter was described that allows to perform reference measurements in the absence of the force caused by the plume. In case of thrusters with high throttleability like gridded ion engines, a beam shutter could be dispensable. However, it may not always be desired or practicable to interrupt the operation of the thruster.

Based on previous studies, carbon fiber velvet was proposed as target material because of its very low effective sputter yield. Accordingly, the measurement presented in this paper was performed with this material.

A two-dimensional scan of a perpendicular cross section through the plume contains all information needed for the calculation of the thrust. However, often it is not practicable to perform a two-dimensional scan. Instead, a radial (one-dimensional) scan through the plume, which is much easier to obain, can be used for an estimate of the thrust of the engine. When the forces $F(r)$ along the radial distances $r = 0 \ldots r_{\max}$ from the plume axis of the thruster are measured, the integration

$$F_{\text{thrust}} = \int_0^{r_{\max}} f(r)\, 2\pi r \,\mathrm{d}r \tag{4}$$

yields an estimate under the assumption of a cylindrically symmetric plume. Here, $f(r) = F(r)/A$ is the "differential thrust", i.e. the force per area or momentum flux density, calculated with the help of the target area A. The measurements should extend to the radius $r_{\max}$ from where on no more significant forces are found.

In conclusion, the paper showed that the force probe is a promising diagnostic for thruster plumes.

Acknowledgments

This work was financially supported by the German Aerospace Center (DLR), Project No. 50 RS 1301.

References

[1]D. L. Brown, M. L. R. Walker, J. Szabo, W. Huang, and J. E. Foster, "Recommended Practice for Use of Faraday Probes in Electric Propulsion Testing," *J. Propul. Power*, Vol. 33, 2017, pp. 582–613.

[2]Z. Zhang, H. Tang, Z. Zhang, J. Wang, and S. Cao, "A retarding potential analyzer design for keV-level ion thruster beams," *Rev. Sci. Instr.*, Vol. 87, 2016, p. 123510.

[3]M. Celik, O. Batishchev, and M. Martnez-Snchez, "Use of emission spectroscopy for real-time assessment of relative wall erosion rate of BHT-200 hall thruster for various regimes of operation," *Vacuum*, Vol. 84, 2010, pp. 1085–1091.

[4]M. Matsui, S. Yokota, H. Takayanagi, H. Koizumi, K. Komurasaki, and Y. Arakawa, "Plume Characterization of Plasma Thrusters Using Diode-Laser Absorption Spectroscopy," in *44th AIAA Aerospace Sciences Meeting and Exhibit, Reno, Nevada, USA*, 2006, p. AIAA–2006–767.

[5]R. Spektor, K. D. Diamant, E. J. Beiting, Y. Raitses, and N. J. Fisch, "Laser induced fluorescence measurements of the cylindrical Hall thruster plume," *Phys. Plasmas*, Vol. 17, 2010, p. 093502.

[6]A. Spethmann, T. Trottenberg, and H. Kersten, "Instrument for spatially resolved simultaneous measurements of forces and currents in particle beams," *Rev. Sci. Instr.*, Vol. 86, 2015, p. 015107.

[7]G. Makrinich and A. Fruchtman, "Enhanced momentum delivery by electric force to ions due to collisions of ions with neutrals," *Phys. Plasmas*, Vol. 20, 2013, p. 043509.

[8]A. Spethmann, T. Trottenberg, and H. Kersten, "Measurement of the Momentum Flux in an Ion Beam," in *32nd International Electric Propulsion Conference, Wiesbaden, Germany*, 2011, p. IEPC–2011–232.

[9]A. Spethmann, T. Trottenberg, and H. Kersten, "Spatially Resolved Momentum Flux Measurements for Thruster Plume Diagnostics," in *33rd International Electric Propulsion Conference, Washington, D.C., USA*, 2013, p. IEPC–2013–079.

[10]A. Spethmann, T. Trottenberg, and H. Kersten, "Measurement and simulation of the momentum transferred to a surface by deposition of sputtered atoms," *Eur. Phys. J. D*, Vol. 70, 2016, p. 255.

[11]T. Trottenberg, A. Spethmann, and H. Kersten, "An Interferometric Force Probe for Thruster Plume Diagnostics," in *34th International Electric Propulsion Conference, Kobe, Japan*, 2015, p. IEPC–2015–419.

[12]A. Spethmann, T. Trottenberg, H. Kersten, F. G. Hey, L. Grimaud, and S. Mazouffre, "Application of Force Measuring Probes for the Investigation of Sputtering and as Diagnostic for HEMP and Hall Thrusters," in *35th International Electric Propulsion Conference, Georgia, Atlanta, USA*, 2017, p. IEPC–2017–245.

[13]D. Bock, A. Spethmann, T. Trottenberg, H. Kersten, and M. Tajmar, "Application of Force Measuring Probes for the Investigation of Sputtering and as Diagnostic for HEMP and Hall Thrusters," in *35th International Electric Propulsion Conference, Georgia, Atlanta, USA*, 2017, p. IEPC–2017–391.

[14]K. Thurner, P.-F. Braun, and K. Karrai, "Fabry-Prot interferometry for long range displacement sensing," *Rev. Sci. Instr.*, Vol. 84, 2013, p. 095005.

[15]K. Thurner, P.-F. Braun, and K. Karrai, "Absolute distance sensing by two laser optical interferometry," *Rev. Sci. Instr.*, Vol. 84, 2013, p. 115002.

[16]U. Minoni, L. Rovati, and F. Docchio, "Absolute distance meter based on a frequency-modulated laser diode," *Rev. Sci. Instr.*, Vol. 69, 1998, pp. 3992–3995.

[17]U. Minoni, E. Sardini, E. Gelmini, F. Docchio, and D. Marioli, "A high-frequency sinusoidal phase-modulation interferometer using an electro-optic modulator: Development and evaluation," *Rev. Sci. Instr.*, Vol. 62, 1991, pp. 2579–2583.

[18]A. Spethmann, T. Trottenberg, and H. Kersten, "Measurement and simulation of forces generated when a surface is sputtered," *Phys. Plasmas*, Vol. 24, 2017, p. 093501.

[19]J. Rutscher, T. Trottenberg, and H. Kersten, "An instrument for direct measurements of sputtering related momentum transfer to targets," *Nucl. Instr. and Meth. B*, Vol. 301, 2013, pp. 47–52.

[20]T. Trottenberg, V. Schneider, and H. Kersten, "Measurement of the force on microparticles in a beam of energetic ions and neutral atoms," *Phys. Plasmas*, Vol. 17, 2010, p. 103702.

[21]A. Spethmann, T. Trottenberg, and H. Kersten, "Measurement of Forces Due to Sputtering of Solid Surfaces," in *34th International Electric Propulsion Conference, Kobe, Japan*, 2015, p. IEPC–2015–236.

[22]T. Trottenberg, J. Rutscher, and H. Kersten, "Experimental Investigation of Momentum Transfer to Solid Surfaces by the Impact of Energetic Ions and Atoms," in *33rd International Electric Propulsion Conference, Washington, D.C., USA*, 2013, p. IEPC–2013–329.

[23]L. D. Landau and E. M. Lifshitz, *Theory of Elasticity – 3rd ed. (Course of Theoretical Physics, Vol. 7)*. Elsevier, 1986.

[24]J. B. Wachtman and D. G. Lam Jr., "Young's Modulus of Various Refractory Materials as a Function of Temperature," *J. American Ceramic Society*, Vol. 42, 1959, pp. 254–260.